NANOSYSTEMS: PHYSICS, CHEMISTRY, MATHEMATICS, 2016, 7 (1), P. 244–252

ERP study of graphite oxide thermal reduction: the evolution of paramagnetism and conductivity

M. V. Gudkov, V. P. Melnikov

Semenov Institute of Chemical Physics, Moscow, Russia

gudkovmv@gmail.com, melnikov@center.chph.ras.ru

PACS 76.30.Pk, 76.30.Rn **DOI 10.17586/2220-8054-2016-7-1-244-252**

The evolution of paramagnetic centers (PMC) and conductivity of graphite oxide (GO) during its thermal reduction has been studied by electron paramagnetic resonance (EPR) at 150 and 165 °C. The GO samples for the study were prepared by systematically varying the $KMnO_4$/Graphite weight ratios in the oxidation reaction. It has been shown that the PMC concentration increase in GO correlates with the intense evolution of gaseous products originating from the former oxygen-containing species of GO. The PMC concentration decrease has been described by the kinetic equation of the first order with an effective k_e and an activation energy value of 33 kcal/mol. The values of k_e decreased with increasing the quantities of $KMnO_4$ used in graphite oxidation reaction. The changes in GO conductivity were followed by measuring the microwave power absorption in the EPR-spectrometer resonator. The conductivity changes correlated with the decay of the radicals and occurred after the decomposition of the oxygen-containing groups was complete.

Keywords: electron paramagnetic resonance, graphite oxide, conductivity, paramagnetic centers, reduction.

Received: 20 November 2015

1. Introduction

The interest in graphite oxide (GO), first synthesized in 1859 [1], has immensely grown in the last decade due to the discovery of graphene's unique properties [2]. The key factors explaining the burst of interest to GO are: (i) simplicity of GO synthesis; (ii) capability of GO to breaking down to few- and even mono-layer particles in proper liquid media; and (iii) practical feasibility of mass production of graphene-like materials from GO by thermal or chemical treatment of the latter. The GO-based materials have already been employed as thin transparent conductive layers, sensors, batteries and capacitors electrodes, etc. [3]. Numerous experimental and theoretical studies have been published regarding GO synthetic procedures, its molecular structure, optimizing the GO reduction and studying the properties of the reduced GO (rGO). The nature of the oxygen-containing groups as well as their formation during the thermal and/or chemical reduction of GO have been investigated with the aid of spectroscopic (IR, Raman, XPS, NMR) and analytical (elemental analysis, XRD, TGA) methods [4]. Owing to their importance in many potential applications, the electrophysical properties of GO-based materials have received much attention recently. In a kinetic study of the monolayer sheet rGO's conductivity, it has been shown [5] that when raising the GO reduction temperature to 200 °C, the conductivity of the product was increased by 3 orders of magnitude. Such conductivity growth infers that polyconjugation of the C=C bonds system was effectively restored during the course of GO reduction. It is also known that under such thermal conditions, the oxygen-containing groups of GO undergo a rapid exothermic decomposition with the release of gaseous CO_2, CO and H_2O. However, despite much work having already been done to formulate the mechanisms for GO reduction, these potential mechanisms remain a matter of debate and,

in particular, the sequence of steps in chemical reactions or the restructuring of the carbon framework during chemical and thermal treatment of GO still need to be clarified [6-8].

Different samples of GO have been studied by EPR and it has been shown that the paramagnetic centers residing on GO are represented by some localized states and, probably, by dangling bonds. It has also been shown that the concentration of the PMC tends to decrease over the course of thermal or chemical GO reduction processes [9-11].

In the present work, with the aid of EPR spectroscopy measurements at 150 and 165 °C, we have followed the evolution of the PMC in the samples of GO having different degrees of oxidation. The temperature interval for the study was chosen based on the results of our earlier volumetric kinetic study of the gaseous products that were released during the thermally stimulated decomposition of GO and are closely associated with the emission of the oxygen-containing functional groups residing on GO [12]. At the initial stage of thermal treatment, when oxygen-containing groups are undergoing vigorous decmposition, the concentration of PMC was found to increase. Under further heating, a reduction of the PMC concentration was observed. Since the emergence and/or increase in an analyte's conductivity brings about an excess absorption of microwaves within EPR resonator, EPR spectrometry was used in this work to measure the variance of electro conductivity for different GO samples. Accordingly, an apparent correlation between the PMC concentration decay and the growth of GO conductivity has been found. The obtained results infer that radical reactions take an active role in the thermally stimulated reduction of GO.

2. Experimental

2.1. Materials

Graphite powders having the particles size in the range of 10 – 20 μm (ash content $<$1.0 %) were used throughout this study. Sulfuric acid (94 %), $NaNO_3$, $KMnO_4$, water and H_2O_2 (3 % water solution) used for GO preparations all had a Reagent Grade purity.

2.2. Preparation of GO

The samples of graphite were oxidized to various predetermined extents via the methods of Hummers [13, 14]. In the standard procedure, 2 g of particulate graphite was charged into a solution of 1 g of $NaNO_3$ in 46 ml of H_2SO_4 and stirred for 60 minutes at room temperature. Then, the reactor was placed into an ice bath and, under vigorous stirring, a measured quantity of $KMnO_4$ (3.0, 4.0, 5.0 or 6.0 g) was charged to the suspension in small portions. Thus, in different experiments, the samples of GO with different degrees of oxidation were provided (the samples labeled GO15, GO20, GO25 and GO30, respectively). Upon completion of the permanganate introduction, the reactor temperature was raised to 35 – 40 °C, and stirred at that temperature for additional 30 – 40 minutes. After diluting the reaction mixture with water followed by treatment with hydrogen peroxide, the oxidized graphite was repeatedly washed with distilled water until a GO/water paste having neutral pH was obtained. The resulting paste was freeze-dried in the form of balls (diameter of $\sim$ 2 – 3 mm) followed by further vacuum drying at 70 °C. The dried paste was then stored in a sealed container.

2.3. ERP spectroscopy

EPR spectra were acquired with the aid of an EPR-B spectrometer (ICP RAS, X-range) at microwave power less than 2 mW and RF amplitude modulation of 0.1 – 0.2 mT. A small sample of MgO with Mg^{2+} ions was kept in the spectrometer resonator as a lateral calibration standard. For the experiment, a GO sample (2.5 – 3.5 mg) was placed in a short thin-walled

glass capillary (inner diameter of ∼1 mm) which in turn was placed in a glass ampule having a vacuum joint, the inner diameter of which was close to the outer diameter of the capillary, thus providing precise centering of the sample in the resonator. A pre-vacuumed sample was placed in the thermostat and was held at a constant temperature for a preset period of time (30 – 60 min in different experiments). Before acquiring the spectrum, the sample was subjected to vacuum again to remove the gaseous products.

Registration of the EPR spectrum involved presetting the microwave channel of the spectrometer so that the input to the synchronous detector reference and the reflected power from the resonator balanced each other, the synchronous detector current would thus be zero. When placed into the resonator, the sample absorbs the microwave radiation and a mismatch occurs, producing a synchronous detector current, which is observed and is proportional to the power absorbed by the sample. Thermal reduction of GO leads to lowering of the sample's resistance and the sample begins to absorb microwave radiation. The registration of the EPR spectra proceeds under changing conditions. The changes in the spectra were then corrected for the corresponding signal intensity changes of the lateral standard which was present in the resonator throughout analysis. At the same time, the detector current allows one to estimate the change in the conductivity of GO samples during heating. The conductivity measurement procedure had several steps. In the first step, the ampule with a pristine GO sample was placed in the spectrometer resonator and the power within the microwave tract was adjusted by the attenuator to the desired level. When one cycle of thermal treatment was finished, the sample was cooled to room temperature and then inserted into the spectrometer resonator again. Shortly after the attenuator was reset to the predetermined position, the detector current was observed and fixed. After readjustment, the EPR spectrum was recorded. The above procedure was repeated after every thermal treatment cycle. Thus, in every experiment, not only an EPR spectrum was acquired but also the conductivity variability was registered for GO thermal treatment. The total value of the absorbed power was obtained by summing the detector currents. The power absorbed due to the electro conductivity was divided by the weight of the sample. Obviously, the initial conductivity magnitude taken as the zero at the start of the experiments differed from sample to sample, and, therefore, the registered values of emergence and conductivity increase should be treated only as relative (not absolute) ones.

3. Results and discussion

The GO samples, characterized by different degrees of oxidation, did provide rather similar EPR spectra. In general terms, these are represented by slightly asymmetric singlets having the line width of 2 – 2.5 G, similar to that described in [9]. Comparison of GO samples having various oxidation degrees (Fig. 1) shows that, with increased oxidation, the initial PMC concentration in GO decreases by 4- to 5-fold. Note the high concentration of the localized PMC in the samples amounting to $\sim 10^{18}$ g^{-1}. The latter high value may infer that the PMC can effectively form and be accumulated in GO starting from the very early stages of the oxidation process and, hence, the dependences depicted in Fig. 1 may represent only the falling branch of the whole graphite oxidation process.

Figure 2 below shows two sets of experimental kinetic curves depicting the change of PMC concentration depending on time for the samples of GO subjected to reduction at 150 and 165 °C. It can be seen that (i) indeed, both the formation and the decay of PMC can proceed during the thermal GO treatment at these temperatures; and (ii) in the samples of GO characterized by different oxidation degrees, the processes for PMC accumulation or decay proceed differently. During the initial stage, a significant increase of the PMC concentration was observed for all samples except GO15, the latter being characterized by the lowest oxidation

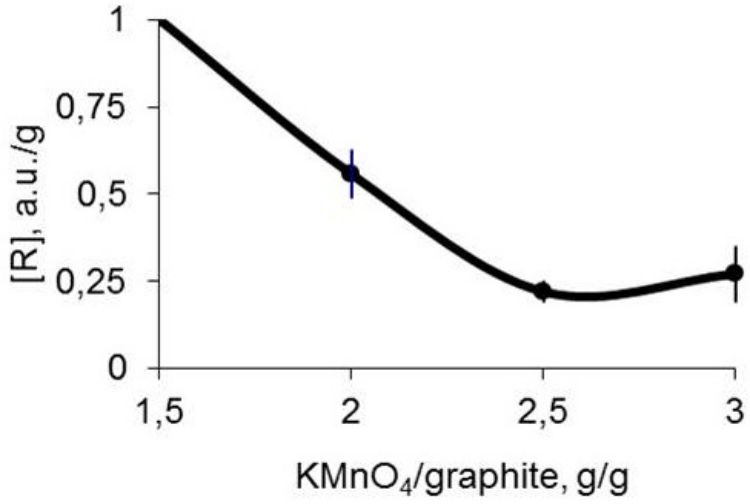

FIG. 1. The dependence of relative PMC concentration in GO samples (two series of measurements) on the relative amount of potassium permanganate used in the oxidation process. The value $[R] = 1$ corresponds to PMC concentration of about $3{\cdot}10^{18}$ g^{-1}

level. The PMC concentration in GO15 began to decrease either from the very beginning of the thermal treatment (at 165 °C) or after a short delay (at 150 °C).The ratio of the maximum PMC concentration to the initial one for both temperatures was found to be in the range of 2.3 – 2.6 for GO20, 3.8 – 4.5 for GO25 and 3.8 – 3.9 for GO30. From the data shown in Fig. 2, it also follows that, with increased GO oxidation levels, the time needed to reach the maximum PMC concentration also increases while PMC decay are processes markedly decreased.

The falling branches of the curves shown in Fig. 2 above are presented in Fig. 3a in different coordinates, $\ln[R]/t$. This new representation of the data shows that the PMC decay is described by a first order kinetic equation. The corresponding calculated values for the effective rate constants are shown at Table 1.

TABLE 1. Values of the effective rate constant

Sample	Ke_e10^3, s^{-1}	
	150 °C	165 °C
GO15	0.23	0.95
GO20	0.16	0.58
GO25	0.13	0.52
GO30	–	–

The data shown in Fig. 3b permits evaluation of Arrhenius parameters for PMC decay processes in GO since the straight line connecting the two temperature points is close to parallel. The evaluation gives an activation energy of, E_a, of $\sim 33 \pm 2$ kcal/mol and a pre-exponential factor, $\lg A$ (s^{-1}), value of $\sim$ 12.8 – 14.2. The kinetic aspects of GO reduction processes have been addressed in a few papers only. In one of the above-mentioned works [5], the kinetics of resistance changes and a thermo-programmed desorption of gaseous products have been studied for a monolayer GO. The activation energy values calculated in that work were found to be $38{\pm}1$ and $32{\pm}4$ kcal/mol. Furthermore, the activation energies values of 38.1 and 32.5 kcal/mol

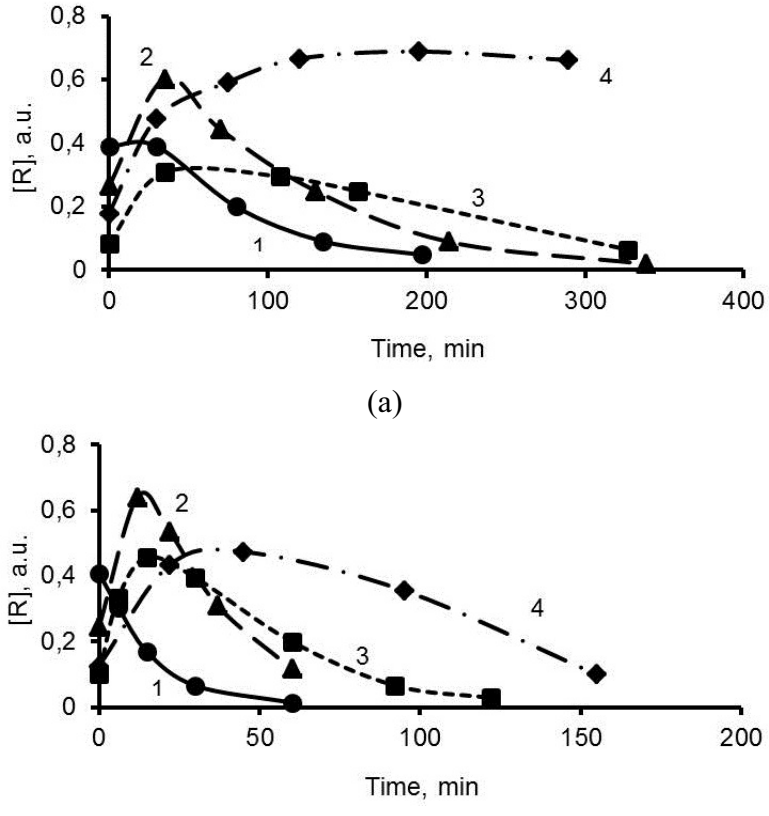

FIG. 2. The changes of PMC concentration depending on time as measured for different GO samples subjected to thermal treatment at 150 (a) and 165 °C (b). Curves 1 – 4 represent the samples GO15, GO20, GO25, GO30, respectively

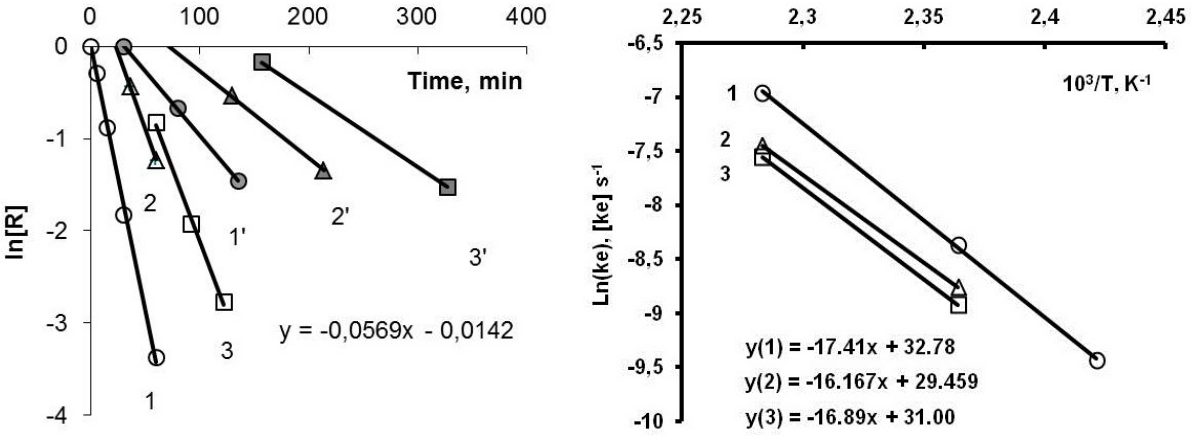

FIG. 3. Linear anamorphoses of kinetic curves for PMC decay in different samples (a) and the Arrhenius-type dependences of the effective rate constants for corresponding temperatures (b). Line numbers correspond to samples 1, 1' – GO15, 2, 2' – GO20, 3, 3' – GO25

have been reported in another work [15], where thermogravimetric analysis (TGA) data were used for calculations based on diffusion and autocatalytic models for the GO reduction process respectively. In yet another paper [16], an activation energy of 40 kcal/mol has been found based on differential scanning calorimetry (DSC) data interrelating the maximum heat release temperature and the heating rate. Our results are in good agreement with those reported in the literature.

The curves in Fig. 4 depict the observed time dependence of the PMC concentration and that of relative conductivity for different GO samples. The electro conductivity detection, or rather, the conductivity increase of the sample GO15 having the lowest oxidation degree is observed at the initial stage of thermal treatment together with the PMC concentration decrease. The match of the observed conductivity initiation with PMC concentration decrease is also seen for the samples GO20 and GO25, which suggests the existence of a relationship between these two processes. In the case of GO30, which has the highest oxidation degree among all samples, no absorption of microwave power that could be related with the emergence of conductivity was observed. Moreover, the decay of PMC centers at 165 °C proceeds much more slowly in this case than for other samples. Also, the PMC concentration at 150 °C remained at the same level for a long time during treatment, thus qualitatively distinguishing it from other samples.

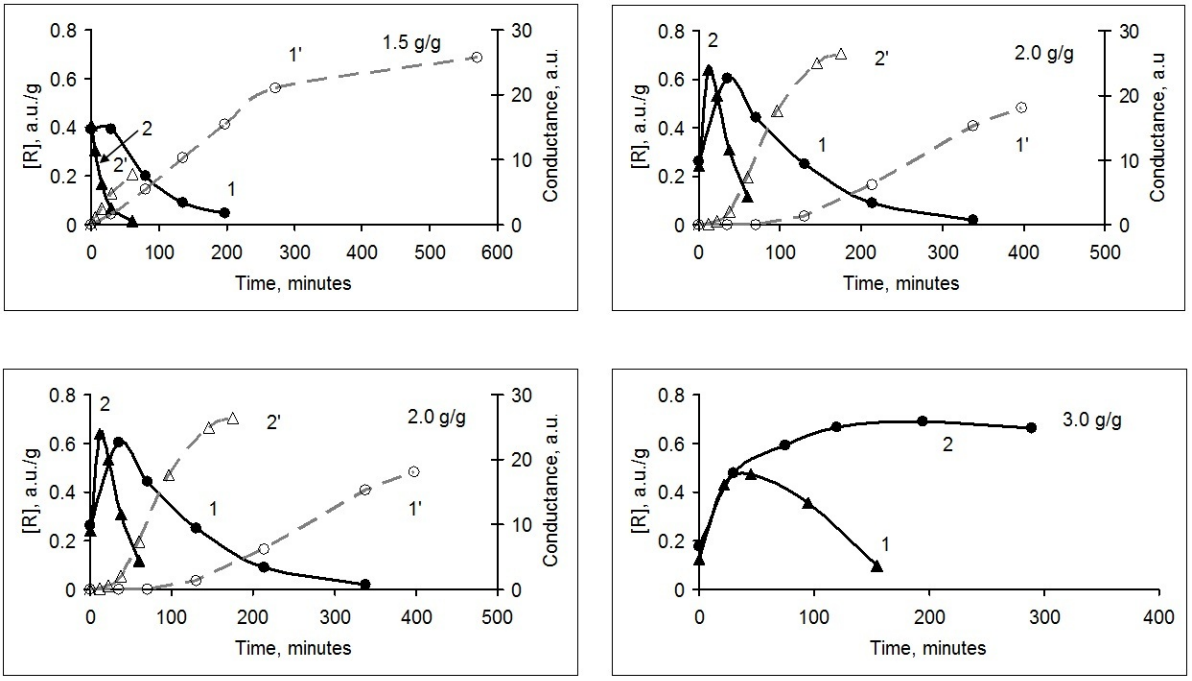

FIG. 4. The dependence of PMC concentration (1, 2) and the relative conductivity (1', 2') of the samples upon the time of heat treatment at two different temperatures of 150 °C (1) and 165 °C (2)

From the very outset of permanganate oxidation, the originally well conductive plane of a single sheet of graphite (consisting almost entirely of sp^2-hybridized polyconjugated carbons) becomes more and more populated with different oxygen-containing moieties, chemically emerging at the expense of sp^2-carbons. Thus, eventually more and more carbon atoms within a single "graphene" layer attain sp^3-hybridization, which leads to a gradual loss of the material's conductivity. Investigations of the resulting GO sheets with the aid of scanning transmission electron microscopy (STEM) and scanning tunneling microscopy (STM) have shown that GO

layer consists of chaotically alternating clusters of oxidized (sp^3) carbons and practically unaffected by oxidation (sp^2) carbon clusters [17-19]. By estimates of various authors based on the intensity ratio of D and G bands in the Raman spectra, the average size of such clusters is around 2.5 – 6.0 nm. It has been noted [20] that the size of these clusters has remained actually the same independently of the thermal or chemical GO reduction mode subsequently employed. The electrical conductivity of graphene (graphite) is attained by virtue of regaining the effective polyconjugation (which was impaired due to oxidation), and hence the GO reduction must be associated with the formation of percolation channels for connecting the separated sp^2-hybridized domains. Our results suggest that the conductivity recovery is associated with the decay of localized paramagnetic states. It is known that the translational mobility is needed for recombination of unpaired electrons, but the implementation mechanism for this process in GO is not clear. It can be assumed that an unpaired electron's motion becomes feasible owing to thermally-assisted transition (hopping) of the electron onto the conjugation domain with subsequent migrating along the latter. Mono- or bi-molecular processes obey first order kinetic equations. For bi-molecular reactions, it is true only in those cases when the second reactant is present in considerable excess relative to that observed. Under these assumptions, the increase in the graphite oxidation level should lead to a lessening in the total area of polyconjugated carbon domains, that is, the oxidation diminishes the concentration of polyconjugated sites which are potential acceptors of unpaired electrons. This, in turn, leads to lowering the effective rate constants of the radical decay.

The number of the oxygen-containing functional groups in GO is a measure of the oxidation degree of the graphite. In an attempt to quantify this parameter, we have used gas volumetry [12]. The method consisted of collecting and segregating the well-known gaseous products (CO_2, CO and H_2O) that are released during the thermal treatment of GO at temperatures up to 250 °C, as well as measuring the partial pressures of the gases in a constant volume, i. e., determining the number of moles of each product per the weight of the GO sample (Fig. 5).

The data in Fig. 5 show that the incremental addition of each extra portion of $KMnO_4$ (0.5 g) resulted in an increase in the total amount of released gaseous products from 4.8 (GO15) to 8.7 (GO20), 10.4 (GO25) and finally to 10.7 (GO30) mmol/g, respectively. The first portion of 1.5 g potassium permanganate introduced per 1 g of the graphite has been consumed with rather low efficiency (it was difficult to initiate graphite oxidation). Addition of the next 0.5 g portion of permanganate (GO15→GO20) gave an additional 3.9 mmol/g of oxygen-containing functional groups. Under further incremental additions of $KMnO_4$ oxidative effectiveness of the latter was progressively lowering: GO20→GO25 – 1.7 mmol/g, GO25→GO30 – 0.3 mmol/g. The significant increase in the oxidation efficiency seen after the addition of the second $KMnO_4$ portion (GO15→GO20) may be associated with both physical (facilitated access of oxidant into the interlayer space of graphite) and chemical (increased reactivity of the carbon atoms neighboring the oxidized sites) reasons. The fact that GO sheet surface consists of sporadically spread, strongly-oxidized domains and those unaffected by the oxidation [17-19] provides evidence in favor of the chemical causes. Indirectly, this hypothesis is also supported by the increased reactivity of the carbon atoms located nearby the deformed regions of the graphene sheet, that has been observed experimentally [21].

Figure 5 shows that the largest decrease of the effective radical decay constant is observed when switching from GO15 to GO20, which coincides exactly with the significant in the degree of functionalization for the graphene sheet's surface. Further changes of the effective radical decay constant for the GO20 to GO25 transition were less pronounced because only comparatively small increase in the degree of functionalization of the graphene sheet occurred

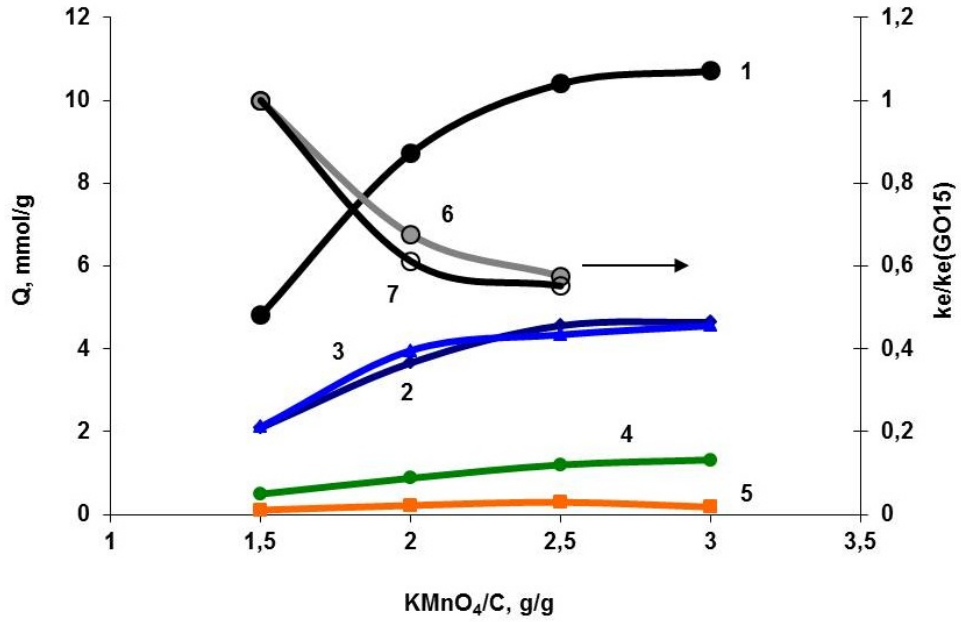

FIG. 5. The yield of typical gaseous products released in the result of thermal reduction of GO by heating the latter at 200 °C: 1 – the total amount of gaseous products, 2 – CO_2, 3 – H_2O, 4 – CO, 5 – unknown impurity. The change of the relative effective radical decay constant on the severity of oxidation of graphite (the amount of $KMnO_4$, used for graphite oxidation): 6 – at 150 °C, 7 – at 165 °C

at that time. The next increment in the degree of oxidation (sample GO30), having only an insignificant effect on the released gas products leads to a qualitative change: the rate of free radical decay abruptly slows down and the emergence of the electrical conductivity is not detected. This is consistent with the observations of Hummers [13, 14], who pointed out that the use of 3 g of potassium permanganate per 1 g of graphite is optimal for thorough oxidation and the use of an additional amount of oxidizing reagent would be unnecessary.

4. Conclusion

The functional groups arising during graphite oxidation on the periphery as well as on the basal surface of graphene particles emerge arise via the formation of covalent C–O bonds, the new bond formation inevitably accompanied by the appearance of an unpaired electron (PMC) at one of the three neighboring carbon atoms. It is possible that such paramagnetic centers can then participate in certain chemical reactions that take place during the oxidation process, thus justifying the decrease in the PMC concentration observed with increased oxidation. At the early stages of graphite oxidation, these unpaired electrons can be capable of migrating through the polyconjugated sp^2-carbon system and have a good chance to recombine since the system is still not badly damaged. At deeper stages of oxidation, when more and more former sp^2-carbon atoms have been transformed to oxygen-containing functionalities and thus have attained sp^3 hybridization, the above opportunities are lost and the unpaired electrons are stabilized. The growth of PMC content at the initial stages of heat treatment, at temperatures providing the intense release of gaseous decomposition products originating from the oxygen-containing functionalities of GO, reveals the important role of the homolytic bond cleavage during the GO reduction process. Further behavior of the PMC (e.g., their decay under continuing thermal treatment) correlates with the incidence of electrical conductivity that has been detected by

the absorption of microwave radiation in the EPR spectrometer resonator. At the moment, it is difficult to give priority to any single mechanism among all possible ones explaining this relationship. From one side, it well may be a transfer (hopping) of the localized state onto a polyconjugated domain of GO, the migration through the polyconjugation system and the recombination. Alternatively, the occurrence of electrical conductivity may also be induced by the transition of the unpaired electron in the conduction band and by the increase in the carrier number. However, the results of the present work provide evidence that the thermal GO reduction process consists of several consecutive stages and proceeds through intermediates which give rise to paramagnetic states.

References

[1] Brodie B.C. On the atomic weight of graphite. *Philos. Trans. R. Soc. London*, 1859, **149**, P. 249–259.
[2] Novoselov K.S., Geim A.K., Morozov S.V., Jiang D., Zhang Y., Dubonos S.V., Grigorieva I.V., Firsov A.A. Electric Field Effect in Atomically Thin Carbon Films. *Science*, 2004, **306**, P. 666–669.
[3] Zhu Y., Murali S., Cai W., Li X., Suk J.W., Potts J.R., Ruoff R.S. Graphene and Graphene Oxide: Synthesis, Properties, and Applications. *Adv. Mater.*, 2010, **22**, P. 3906–3924.
[4] Singh V., Joung D., Zhai L., Das S., Khondaker S.I., Seal S. Graphene based materials: Past, present and future. *Progress in Materials Science*, 2011, **56**, P. 1178–1271.
[5] Jung I., Field D.A., Clark N.J., Zhu Y., Yang D., Piner R.D., Stankovich S., Dikin D.A., Geisler H., Ventrice C.A., Ruoff J.R.S. Reduction Kinetics of Graphene Oxide Determined by Electrical Transport Measurements and Temperature Programmed Desorption. *J. Phys. Chem. C*, 2009, **113**, P. 18480–18486.
[6] Chua C. K., Pumera M. Covalent Chemistry on Graphene. *Chem. Soc. Rev.*, 2013, **42**(8), P. 3222–3233.
[7] Acik M., Mattevi C., Gong C., Lee G., Cho K., Chhowalla M., Chabal Y.J. The Role of Intercalated Water in Multilayered Graphene Oxide. *ACS Nano*, 2010, **4**, P. 5861–5868.
[8] Zhan D., Ni Z., Chen W., Sun L., Luo Z., Lai L., Yu T., Wee A.T.S., Shen Z. Electronic Structure of Graphite Oxide and Thermally Reduced Graphite Oxide. *Carbon*, 2011, **49**, P. 1362–1366.
[9] Ćirićc L., Sienkiewicz A., Gaál R., Jaćimović J., Vâju C., Magrez A., Forró L. Defects and Localization in Chemically-Derived Graphene. *Phys. Rev. B*, 2012, **86**, P. 195139.
[10] Ali F., Agarwal N., Nayak P.K., Das R., Periasamy N. Chemical Route to The Formation of Graphene. *Current Science*, 2009, **97**, P. 683–685.
[11] Rao S.S., Stesmans A., Wang Y., Chen Y. Direct ESR Evidence for Magnetic Behavior of Graphite Oxide. *Physica E*, 2012, **44**, P. 1036–1039.
[12] Gorshenev V.N., Melnikov V.P. Thermally-assisted expansion of graphites with different degree of oxidation. *Chimicheskaya Physika*, 2013, **32**, P. 37–43. (in Russian)
[13] Hummers W.S. Preparation of Graphitic Acid. United States Patent Office, 1957, 2798878.
[14] Hummers W.S., Offeman R.E. Preparation of Graphitic Oxide. *J. Am. Chem. Soc.*, 1958, **80**, P. 1339.
[15] Barroso-Bujans F., Alegría A., Colmenero J. Kinetic Study of the Graphite Oxide Reduction: Combined Structural and Gravimetric Experiments under Isothermal and Nonisothermal Conditions. *J. Phys. Chem. C*, 2010, **114**, P. 21645–21651.
[16] Yin K., Li H., Xia Y., Bi H., Sun J., Liu Z., Sun L. Thermodynamic and Kinetic Analysis of Low Temperature Thermal Reduction of Graphene Oxide. *Nano-Micro Lett.*, 2011, **3**, P. 51–55.
[17] Erickson K., Erni R., Lee Z., Alem N., Gannett W., Zettl A. Determination of the Local Chemical Structure of Graphene Oxide and Reduced Graphene Oxide. *Adv. Mater.*, 2010, **22**, P. 4467–4472.
[18] Mkhoyan K. A., Contryman A. W., Silcox J., Stewart D.A., Eda G., Mattevi C., Miller S., Chhowalla M. Atomic and Electronic Structure of Graphene-Oxide. *Nano Lett.*, 2009, **9**, P. 1058–1063.
[19] Paredes J.I., Villar-Rodil S., Solıs-Fernandez P., Martínez-Alonso A., Tascón J.M.D. Atomic Force and Scanning Tunneling Microscopy Imaging of Graphene Nanosheets Derived from Graphite Oxide. *Langmuir*, 2009, **25**, P. 5957–5968.
[20] Mattevi C., Eda G., Agnoli S., Miller S., Mkhoyan K. A., Celic O., Mastrogiovanni D., Granozzi G., Garfunkel E., Chhowalla M. Evolution of Electrical, Chemical, and Structural Properties of Transparent and Conducting Chemically Derived Graphene Thin Films. *Adv. Funct. Mater.*, 2009, **19**, P. 2577–2583.
[21] Zhang Y.H., Wang B., Zhang H.R., Chena Z.Y., Zhanga Y.Q., Wanga B., Suia Y.P., Lia X.L., Xiea X.M., Yua G.H., Jinc Z., Liuc X.Y. The Distribution of Wrinkles and their Effects on the Oxidation Resistance of Chemical Vapor Deposition Graphene. *Carbon*, 2014, **70**, P. 81–86.